

Inversionless gain in an optically-dense resonant Doppler-broadened medium

A. K. Popov and S. A. Myslivets

*Institute for Physics, Russian Academy of Sciences, Krasnoyarsk,
660036, Russia*
popov@ksc.krasn.ru

Thomas F. George

*Office of the Chancellor / Departments of Chemistry and Physics &
Astronomy, University of Wisconsin-Stevens Point, Stevens Point,
WI 54481-3897, USA*
tgeorge@uwsp.edu

Abstract: Resonant nonlinear-optical interference processes in four-level Doppler-broadened media are studied. Specific features of amplification and optical switching of short-wavelength radiation in a strongly-absorbing resonant gas under coherent quantum control with two longer wavelength radiations, are investigated. The major outcomes are illustrated with virtual experiments aimed at inversionless short-wavelength amplification, which also address deficiencies in this regard in recent experiments. With numerical simulations related to the proposed experiment in optically-dense sodium dimer vapor, we show optimal condition for optical switching and the expected gain of the probe radiation, which is above the oscillation threshold.

© 2018 Optical Society of America

OCIS codes: (020.1670) Coherent optical effects; (140.4480) Optical amplifiers; (190.4410) Nonlinear optics, parametric processes; (190.4970) Parametric oscillators and amplifiers; (190.5650) Raman effect; (190.7220) Upconversion; (200.4740) Optical processing.

References and links

- [†] Ossipov Russian Folk Orchestra, conducted by Nikolai Kalinin, “Ochi Chornyje” ©1994 CD Ltd.
 [‡] Thomas F. George, piano, Michael Kaupa, trumpet/flügelhorn, “Close Your Eyes” ©1995 Hester Park, <http://www.uwsp.edu/admin/chancellor/tgeorge/CDreview.htm>
1. M.O. Scully, “Resolving conundrums in lasing without inversion via exact solutions to simple models” *Quantum Optics* **6**, 203-215 (1994).
 2. O. Kocharovskaya and P.Mandel, “Basic models of lasing without inversion: General form of amplification condition and problem of self-consistency,” *ibid.*, 217-230.
 3. B. G. Levi, “Some benefits of quantum interference become transparent,” *Physics Today* **45**, 17-19 (May 1992).
 4. P. Mandel, “Lasing without inversion: a useful concept?” *Contemp. Phys.* **34**, 235-246 (1993).
 5. M. O. Scully and M. Fleischhauer, “Laser without inversion,” *Science* **263**, 337-338 (1994).
 6. A. K. Popov and S. G. Rautian, “Atomic coherence and interference phenomena in resonant nonlinear optical interactions” (invited paper), in *Coherent Phenomena and Amplification without Inversion*, A. V. Andreev, O. Kocharovskaya and P. Mandel, eds., *Proc. SPIE* **2798**, 49-61 (1996), <http://xxx.lanl.gov/abs/quant-ph/0005114>.
 7. A. K. Popov, “Inversionless amplification and laser-induced transparency at discrete transitions and the transitions to continuum” (review), *Bull. Russ. Acad. Sci., Physics* **60**, 927-945 (1996), <http://xxx.lanl.gov/abs/quant-ph/0005108>.
 8. S. E. Harris, “Electromagnetically induced transparency,” *Physics Today* **50**, 36-42 (July 1997).
 9. A. J. Merriam, S. J. Sharpe, H. Xia, D. Manuszak, G. Y. Yin, and S. E. Harris, “Efficient gas-phase generation of coherent vacuum ultraviolet radiation,” *Opt. Lett.* **24**, 625-627 (1999).

10. S. E. Harris and L. V. Hau, "Nonlinear optics in low light-levels," *Phys. Rev. Lett.* **82**, 4611-4614 (1999).
 11. S. E. Harris and Y. Yamamoto, "Photon switching by quantum interference," *Phys. Rev. Lett.* **81**, 3611-3614 (1999).
 12. M. D. Lukin, A. V. Matsko, M. Fleischhauer, and M.O. Scully, "Quantum noise and correlations in resonantly enhanced wave mixing based on atomic coherence," *Phys. Rev. Lett.* **82**, 1847-1850 (1999).
 13. U. Hinze, L.Meyer, B. N. Chichkov, E. Tiemann, and B. Wellegehausen, "Continuous parametric amplification in a resonantly driven double- Λ system," *Opt. Commun.* **166**, 127-132 (1999).
 14. A. K. Popov and S. A. Myslivets, "Resonant four-wave frequency mixing in Doppler-broadened transitions," *Quantum Electron.* **27** 1004-1008 (1997), <http://turpion.ioc.ac.ru/>.
 15. A. K. Popov, "Interference at quantum transitions: lasing without inversion and resonant four-wave mixing in strong fields at Doppler-broadened transitions," in *Nonlinear Optics*, Sergei G. Rautian, Igor M. Beterov and Natalia M. Rubtsova, eds., *Proc. SPIE* **3485**, 252-263 (1998), <http://xxx.lanl.gov/abs/quant-ph/0005118>.
 16. T. Ya. Popova, A. K. Popov, S. G. Rautian, and R. I. Sokolovskii, "Nonlinear interference effects in emission, absorption, and generation spectra," *JETP* **30**, 466 (1970) [Translated from *Zh. Eksp. Teor. Fiz.* **57** 850, (1969)], <http://xxx.lanl.gov/abs/quant-ph/0005094>.
 17. T. Ya. Popova, A. K. Popov, "Effect of resonance radiative processes on the amplification factor," *Zhurn.Prikl. Spektrosk.*, **12**, No 6, 989, (1970) [Translated in Engl.: *Journ. Appl. Spectr* **12**, No 6, 734, (1970)], <http://xxx.lanl.gov/abs/quant-ph/0005047>.
 18. T. Ya. Popova, A. K. Popov, "Shape of the amplification line corresponding to an adjacent transition in a strong field," *Izv.Vysh. Uchebn. Zaved., Fizika* No 11, 38, (1970) [Translated in Engl.: *Soviet Phys. Journ.* **13**, No 11, 1435, (1970)], <http://xxx.lanl.gov/abs/quant-ph/0005049>.
 19. A. K. Popov, *Introduction in Nonlinear Spectroscopy*, Nauka, Novosibirsk, 1983, 274p. (in Russ).
 20. I. M. Beterov, "Investigation on nonlinear resonant interaction of optical fields in three-level gas laser," *Cand. Sci. Dissertation*, Institute of Semiconductor Physics SD USSR AS, Novosibirsk, Dec. 1970.
 21. A. K. Popov, S. A. Myslivets, E. Tiemann, B. Wellegehausen and G. Tartakovskiy, "Quantum interference and Manley-Rowe relations at resonant four-wave mixing in optically-thick Doppler-broadened Media," *JETP Lett.* **69**, 912-16 (1999), <http://ojps.aip.org/jetplo/>.
-

1 Introduction

Coherent quantum control (CQC) of optical processes have proven to be a powerful tool to manipulate refraction, absorption, transparency, gain and conversion of electromagnetic radiation (for a review, see [1, 2, 3, 4, 5, 6, 7, 8]). Among recent achievements are the slowing down of the light group speed to a few m/s, highly-efficient frequency conversion, squeezed quantum state light sources and optical switches for quantum information processing [9, 10, 11, 12]. Much interest has been shown in the physics and diverse practical schemes of amplification without inversion (AWI). This present paper is aimed at studying nonlinear coherence and interference effects (NIE) underlying an approach which accounts for the specific features of Doppler broadening of coherently-driven quantum transitions and the inhomogeneous distribution of the power saturated material parameters along the medium. Special emphasis is placed on NIE processes, which would allow converting easily-achievable long-wavelength gain to a higher- frequency interval. Another outcome is the realization of the optical switching of the medium from opaque to amplifying via a transparent state by small variation of the intensity or frequency of one of the coupled radiations. Important features of both the signal and idle radiation produced with the aid of the proposed scheme entail the suppression of quantum noise. We propose potential experiments towards inversionless generation and optical switch based on CQC. The potential and optimum conditions for the realization of such effects in an optically-dense Doppler-broadened medium are explored.

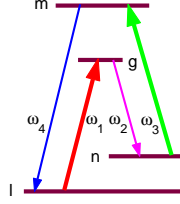


Fig. 1. Energy levels and coupled fields.

2 Resonance coherence and interference processes at Doppler broadened transitions: propagation features and parametric gain

A typical coupling schematic relevant to the topics under discussion and to the experimental situation [13] is depicted in Fig. 1. A weak probe radiation E_4 at frequency ω_4 propagates through an optically-dense Doppler-broadened medium controlled with two longer-wavelength driving radiations E_1 and E_3 at ω_1 and ω_3 . All waves are co-propagating. Owing to four-wave mixing (FWM), the probe wave generates radiation at $\omega_2 = \omega_1 + \omega_3 - \omega_4$ at the transition gn , where the driving field E_1 easily produces a large Stokes gain. Alternatively, the enhanced generated radiation E_2 contributes back to E_4 due to FWM, which dramatically changes the propagation features of the probe field. Therefore, the problem under consideration reduces to the solution of a set of the coupled equations for the four waves $(E_i/2) \exp[i(k_i z - \omega_i t)] + c.c.$ ($i = 1...4$), traveling in an optically-thick medium:

$$dE_{4,2}(z)/dz = i\sigma_{4,2}E_{4,2} + i\tilde{\sigma}_{4,2}E_1E_3E_{2,4}^*, \quad (1)$$

$$dE_{1,3}(z)/dz = i\sigma_{1,3}E_{1,3} + i\tilde{\sigma}_{1,3}E_4E_2E_{3,1}^*. \quad (2)$$

Here $\omega_4 + \omega_2 = \omega_1 + \omega_3$, k_j are wave numbers in a vacuum, $\sigma_j = -2\pi k_j \chi_j = \delta k_j + i\alpha_j/2$, α_j and δk_j are intensity-dependent absorption indices and dispersion parts of the wave numbers, $\tilde{\sigma}_4 = -2\pi k_4 \tilde{\chi}_4$ (etc.) is a FWM cross-coupling parameter, and χ_j and $\tilde{\chi}_j$ are the corresponding nonlinear susceptibilities dressed by the driving fields. An amplification or absorption of any of the coupled radiations influences the propagation features of the other ones. In the approximation that a change of the driving radiations $E_{1,3}$ along the medium is neglected (for example, at the expense of the saturation effects), the system (1)-(2) reduces to two coupled standard equations of nonlinear optics for E_4 and E_2 , whereas the medium parameters are homogeneous along z . If $\Delta k = \delta k_1 + \delta k_3 - \delta k_2 - \delta k_4 = 0$, the input values $I_{4,2} \equiv |E_{4,2}|^2$ at $z = 0$ are $I_{20} = 0, I_{40} \neq 0$ and the absorption (gain) rate substantially exceeds that of the nonlinear optical conversion we obtain at the exit of the medium of the length L :

$$I_4/I_{40} = |\exp(-\alpha_4 L/2) + (\gamma^2/(2\beta)^2) [\exp(g_2 L/2) - \exp(-\alpha_4 L/2)]|^2. \quad (3)$$

Alternatively, if $I_{40} = 0, I_{20} \neq 0$,

$$\eta_4 = I_4/I_{20} = (|\gamma_4|^2/(2\beta)^2) |\exp(g_2 L/2) - \exp(-\alpha_4 L/2)|^2. \quad (4)$$

Here $\gamma^2 = \gamma_2^* \gamma_4$, $\gamma_{4,2} = \chi_{4,2} E_1 E_3$, $\beta = (\alpha_4 - \alpha_2)/4$, ($|\gamma^2|/\beta^2 \ll 1$), and $g_2 \equiv -\alpha_2$. From (3) and (4) it follows that at relatively small lengths the FWM coupling may even increase the depletion rate of the probe radiation, depending on the signs of $Im\gamma_{4,2}$ and $Re\gamma_{4,2}$. In order to achieve amplification, large optical lengths L and significant Stokes gain on the transition gn ($\exp(g_2 L/2) \gg |(2\beta)^2/\gamma^2|$), as well as effective FWM both at ω_2 and ω_4 , are required.

The important feature of the considered far-from-degenerate interaction is that the magnitude and sign of single-photon and multiphoton resonance detunings and, consequently, of the amplitudes and phases of nonlinear polarizations, differ for molecules at different velocities due to the difference in their frequency Doppler shifts. Their interference determined by the interference of elementary quantum pathways, and accounting for Maxwell's velocity distribution and saturation effects, results in a nontrivial dependence of the material macroscopic parameters on the intensities of the driving fields and on the frequency detunings from the Doppler-broadened resonances. The relevant solutions for elements of the density matrix, and consequently for the material parameters in the ED equations (1) and (2), are cumbersome. They are provided in [14, 15], where the solution is found exactly with respect to $E_{1,3}$ and in the first approximation for $E_{4,2}$. The various relaxation processes, Boltzmann excitation of the level n , distribution over rotational sub-levels and dependence on the molecule velocity were taken into account. This allows numerical averaging over the Maxwell velocity distribution as well as further virtual experiments. These formulas are used here for analysis of the dependence of the quantities $\alpha_{4,2}$ and $\gamma_{4,2}$ on the intensities and frequencies of the fields and also to obtain a numerical solution of the system (1)–(2) which accounts for the inhomogeneity of the coefficients and phase mismatch Δk .

3 Numerical simulations

The numerical simulations are done for the transitions $l-g-n-m-l$ (Fig. 1) attributed to those of sodium dimers [Na_2 : $X'\Sigma_g^+(v'' = 0, J'' = 45) - A'\Sigma_u^+(6, 45)(\lambda_1 = 655 \text{ nm}) - X^1\Sigma_g^+(14, 45)(\lambda_2 = 756 \text{ nm}) - B^1\Pi_u(5, 45)(\lambda_3 = 532 \text{ nm}) - X'\Sigma_g^+(0, 45)(\lambda_4 = 480 \text{ nm})$] from the experiment [13] and using experimental relaxation data. The Doppler width of the transition (FWHM) at the wavelength $\lambda_4 = 480 \text{ nm}$ at a temperature of about 450° C is approximately equal to 1.7 GHz. Then the Boltzmann population of level n is about 2% of that of level l . The driving radiations are set at exact resonance with the corresponding transitions ($\Omega_1 = \omega_1 - \omega_{gl} = 0, \Omega_3 = \omega_3 - \omega_{mn} = 0$) and are characterized by the coupling Rabi frequencies $G_1 = E_1 d_{lg}/2\hbar$ and $G_3 = E_3 d_{nm}/2\hbar$. The resonant condition results in strong depletion of the driving radiation E_1 along the medium. We scale the length of the medium L to the absorption length $L_4 = 1/\alpha_{40}$ at $\Omega_4 = \omega_4 - \omega_{ml} = 0$, with all driving fields turned off.

Figures 2(a-c) and the movie mov1a.mov and mov1b.mov display changes in the spectral dependencies of the velocity averaged material parameters with variation of the driving fields. Figure 2(a) is generated for the input Rabi frequencies $G_{10} = 60 \text{ MHz}$ and $G_{30} = 20 \text{ MHz}$. It displays substantial Autler-Townes splitting of the Stokes lineshape with minimum gain in the resonance. Corresponding quantum interference structures appear in the absorption and FWM coupling parameters, which behave quite differently. As it is shown below, maximum gain $I_4(L)/I_{40}$ occurs at $L/L_{40} = 15$, where the driving fields deplete down to $G_1 = 16 \text{ MHz}$ and $G_3 = 19 \text{ MHz}$. This gives rise to a dramatic change in the spectral properties of absorption (upper plot), of the Stokes gain (lower plot) and of the FWM coupling parameters $\gamma_{4,2}$ (Fig. 2b). Due to the interplay of the quantum interference processes and population cycling in the strong fields, absorption at the resonance becomes even larger than in the unperturbed medium. Figure 2(c), computed for $G_1 = 60 \text{ MHz}$ and $G_3 = 80$, displays further feasibility to manipulate material parameters with quantum coherence and interference processes. Figure 3 (a-c) and the movies mov2a.mov and mov2b.mov display AWI in an optically-thick Doppler-broadened medium controlled with injected coherence. Figure 3(a) corresponds to the input intensities, selected for the Fig. 2(a). It shows a substantial gain, provided by the right choice of the optimum optical length and resonance detunings. The virtual experiment displays no gain in the resonance. Due to the interplay of the absorption,

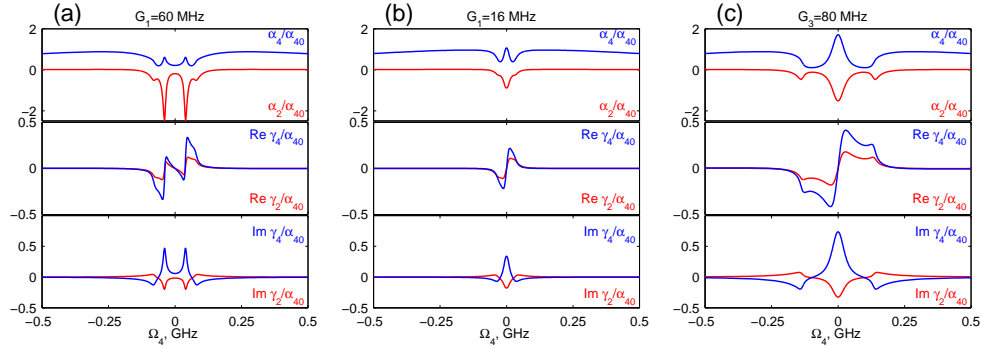


Fig. 2. Intensity-dependent absorption index for the signal radiation, Stokes amplification index for the idle radiation and real and imaginary parts of the FWM cross coupling parameters vs signal frequency resonance detuning. The driving fields are set to the resonance. (a) and (b) – mov1a.mov (2.02MB, audio[†]) ($G_3 = 20$ MHz, G_1 varies); (c) – mov1b.mov (2.03MB, audio[†]) ($G_1 = 60$ MHz, G_3 varies). The current magnitude of the variable Rabi frequency runs at the top of the screen.

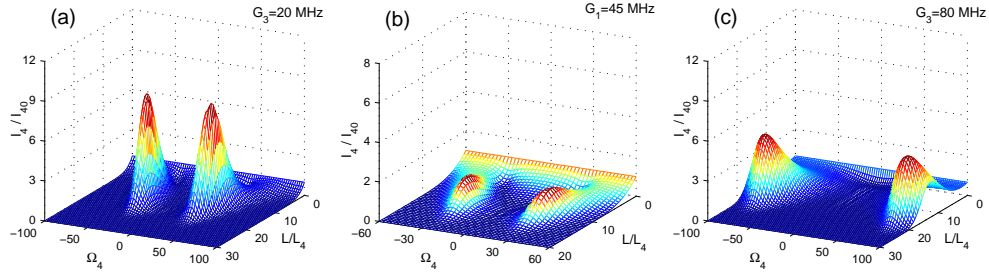


Fig. 3. Inversionless gain in optically thick Doppler-broadened medium. a and c – mov2b.mov (1.50MB, audio[†]) ($G_{10} = 60$ MHz, G_{30} varies); b – mov2a.mov (1.54MB, audio[†]) ($G_{30} = 20$ MHz, G_{10} varies). The current magnitudes of the variable Rabi frequency are displayed at the top of the screen.

Stokes gain and FWM processes as well as depletion of the driving radiation along the medium, the optimum detuning does not correspond to that for the maximum Stokes amplification index at the entrance of the cell (Fig. 2(a)). Figure 3(b) is generated at the minimum input driving intensities required to get the medium transparent. Figure 3(c), which corresponds to the input intensities used for computing Fig. 2(c), shows that an increase in the intensity of the driving field E_3 even decreases the output signal radiation. It is important to note that a very sharp change in the output signal at small variation

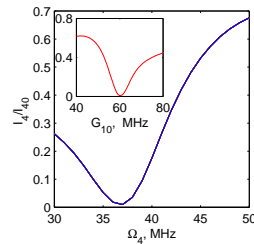


Fig. 4. Optical switch.

of the frequency or the medium length (see, e.g., Fig. 3(a)) or the driving intensities (see the movies mov2a.mov and mov2b.mov) in properly-chosen intervals give rise to dramatic change in the intensity of the transmitted signal. This allows one to realize

optical switching, based on quantum coherence processes. As examples, the upper inset in Fig. 4 is derived from the movies mov2a.mov and mov2b.mov for $G_{30} = 20$ MHz, $\Omega_4 = 37$ MHz and $L/L_{40} = 3$, and the main plot for $G_{10} = 60$ MHz and $G_{30} = 20$ MHz ($L/L_{40} = 4$). The minimum transmission is below 1%. The graphs also show that near the entrance of the cell, parametric coupling even increases the rate of depletion of the probe radiation. Figure 5 presents numerical analysis of the experiment [13]. In the

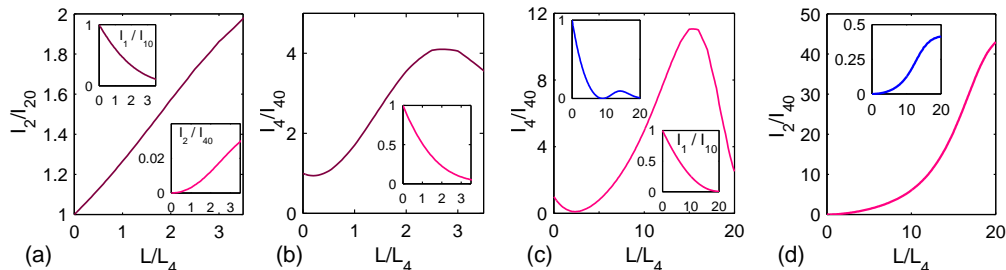


Fig. 5. Numerical simulation of the experiment [13] – (a) and (b), and of the proposed experiment towards inversionless gain – (c) and (d).

experiment all four fields were set in corresponding resonances, the input Rabi frequency at the Stokes transition being about 10 times larger than the probe one. This was in turn assumed for computing Figs.5(a) and 5(b). The upper inset in Fig. 5(a) depicts depletion of the driving radiation E_1 ($G_{10} = 12$ MHz, $G_{30} = 7$ MHz), at the the optical length, corresponding to the experimental value. The computed gain of the Stokes beam (main plot in Fig. 5(a)) as well as that for the probe radiation (main plot in Fig. 5(b)) are in a good agreement with the experimental data. This simulation is aimed at demonstrating that the gain of the probe radiation is derived from FWM with no contribution of the parametric amplification. Parametric amplification in the conditions of this experiment could be achieved by turning off the input Stokes radiation. Indeed, in this case only depletion of the probe radiation (lower inset inset in Fig. 5(b)) and weak output Stokes intensity (lower inset in Fig. 5(a)) come out from the same numerical simulations.

The main plots in the Figs, 5(c,d) are to propose favorable conditions for inversionless amplification. These plots are generated for the input driving Rabi frequencies $G_{10} = 60$ MHz, $G_{30} = 30$ MHz and for the near optimum detuning $\Omega_4 = 35$ MHz. The main plot in Fig. 5(c) displays substantial inversionless amplification, and in Fig. 5(d), generated idle radiation under relatively low input intensities. For the selected transitions a characteristic value of the Rabi frequency of about 80 MHz approximately corresponds to radiation powers in the interval 100 to 200 mW focused on a spot with sizes of about a few parts of a millimeter. In the same conditions, but for the probe field tuned to the resonance (at $\Omega_4 = 0$), gain does not exist and generated idle radiation dramatically decreases (upper insets in Figs. 5(c,d)). All the above presented simulations account for phase mismatch stipulated from the detunings. Both probe and idle radiations are supposed to be weak and unperturbative.

NIE as an origin of the difference in the rates of induced transitions from upper and lower levels and consequently – of AWI were discussed in ref. [16]. The optimum conditions and features of AWI were explored and numerically illustrated for three level V scheme of neon transitions in ref. [17, 18, 19]. Related experiments and evidence of AWI were reported in ref. [20] (for review of the later works see ref. [1, 2, 3, 4, 5, 6, 7, 8]). In order to simplify the proposed experiment we do not assume here a source of incoherent excitation of the medium (the formulas accounting for such excitation are provided in ref. [14, 15]). Therefore the energy acquired by the probe field here is taken

entirely from the driving fields. However we call the effect as inversionless gain, derived from the quantum coherence and interference processes, rather than optical parametric amplification. This is due to the fact that the discussed amplification effect can not be thought as the result of the consequent separate elementary effects of absorption, FWM, Stokes gain and back FWM giving rise to OPA. We want to stress that consideration of these processes separately in a resonant medium is not adequate for the physics of the interference process and, as it has been shown in [21], would result even in qualitatively wrong predictions. The proposed approach based on NIE increases number of the interfering channels for the energy conversion including those through populating of the excited levels, modified Raman-type and parametric processes.

4 Conclusion

In conclusion, this paper considers various optical processes in four-level Doppler-broadened media, controlled with laser injected coherence. The scheme of inversionless amplification and optical switching of short-wavelength radiation in strongly-absorbing resonant four-level gas is proposed. They are controlled with two driving fields at longer wavelengths and become possible due to the optical parametric coupling and readily-achievable Stokes gain. Optimal conditions for the experiment on sodium dimer vapor and the expected gain are explored with the aid of numerical simulations. The relevant driving intensities correspond to focused cw radiation on the order of several tens of mW, i.e., to about one photon per thousand molecules. The analysis shows that further increase of the driving Rabi frequencies up to about 100-200 MHz allows one to achieve the gain above the threshold of mirror-less self-oscillation.

AKP thanks B. Wellegehausen and B. Chichkov for stimulating discussions. We thank the U.S. National Research Council - National Academy of Sciences for support of this research through the international Collaboration in Basic Science and Engineering program. AKP and SAM acknowledge funding support from the International Association of the European Community for the promotion of co-operation with scientists from the New Independent States of the former Soviet Union (grant INTAS-99-19) and Russian Foundations for Basic Research (grant 99-02-39003) and from the Center on Fundamental Natural Sciences at St. Petersburg University (grant 97-5.2-61).